

## Three-Dimensional NOESY-HMQC Spectroscopy of a $^{13}\text{C}$ -Labeled Protein

MITSUHIKO IKURA, LEWIS E. KAY, ROLF TSCHUDIN, AND AD BAX

*Laboratory of Chemical Physics, NIDDK, National Institutes of Health, Bethesda, Maryland 20892*

Received August 29, 1989

The analysis of NMR spectra of medium-size (10–20 kDa) proteins is often difficult because of severe signal overlap. A number of isotope-edited 2D experiments (1–7) and, more recently, 3D NMR experiments have been used to alleviate this problem (8–12). Spreading spectral information in three independent frequency dimensions greatly reduces spectral overlap and thereby simplifies the process of analysis. The heteronuclear 3D experiments (13, 10–12) are particularly useful in this respect, because the total number of resonances remains unchanged relative to the corresponding homonuclear  $^1\text{H}$  2D spectrum; the chemical shift of the heteronucleus is merely used to disperse the resonances in the regular 2D spectrum along a third axis. All applications of heteronuclear 3D experiments to proteins published to date combine the commonly used homonuclear  $^1\text{H}$  experiments NOESY (14, 15) and HOHAHA (16, 17) with the  $^1\text{H}$ -detected heteronuclear multiple-quantum correlation (HMQC) experiment (18–20). Recently, it has been shown that the HMQC experiment does not provide as high a resolution as some more complex pulse sequences (21). However, the resolution in the dimension of the heteronuclear chemical shift is usually limited by digital resolution, and the potentially lower resolution does not play a role. So far, all protein applications of heteronuclear 3D NMR have utilized  $^{15}\text{N}$  as the heteronucleus. Here we report the first use of heteronuclear 3D protein NMR using the  $^{13}\text{C}$  chemical shift to spread the  $^1\text{H}$  resonances.

Although at first sight, the change from  $^{15}\text{N}$  to  $^{13}\text{C}$  may appear simple, there were a number of problems that had made it uncertain whether this approach would be successful. First, the heteronuclear dipolar line-broadening effect of  $^{13}\text{C}$  on the resonance of its directly attached proton(s) is severe, typically causing a twofold increase of the regular proton linewidth. This sharply reduces sensitivity in those 3D experiments where one of the magnetization transfer steps relies on  $^1\text{H}$ - $^1\text{H}$   $J$  coupling. Our experiments with fully (about 95%)  $^{13}\text{C}$ -labeled protein also showed a reduction in the proton  $T_1$  by about 30% relative to the unlabeled protein, and it was not certain a priori whether this strong heteronuclear dipolar relaxation would have a negative influence on the quality of the NOESY spectrum. A second problem arises from the presence of relatively large  $^1J_{\text{CC}}$  couplings, varying from about 60 Hz for  $\text{C}_\alpha$ -carbonyl and aromatic couplings to about 35 Hz for couplings between aliphatic carbons. Attempting to resolve these splittings in the 3D experiment would increase the number of resonances and thus decrease signal-to-noise. As shown by Markley and co-workers (22–24), using a relatively low level of  $^{13}\text{C}$  labeling reduces the  $^{13}\text{C}$ - $^{13}\text{C}$  broaden-

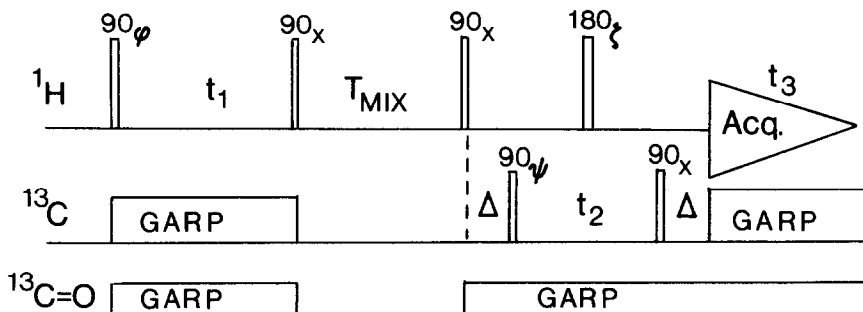


FIG. 1. Pulse scheme of the 3D NOESY-HMQC experiment. The following eight-step phase cycle is used:  $\phi = x, -x$ ;  $\psi = 2(x), 2(-x)$ ;  $\zeta = 4(x), 4(y)$ ; Acq. =  $x, 2(-x), x, -x, 2(x), -x$ . To obtain complex data in the  $t_1$  dimension, the sequence is repeated with  $\phi = y, -y$ , and data are stored separately. To obtain complex data in the  $t_2$  dimension, the above procedure is repeated also for  $\psi = 2(y), 2(-y)$ ;  $90^\circ$  pulse widths used were  $10 \mu\text{s}$  ( $^1\text{H}$ ),  $31 \mu\text{s}$  ( $^{13}\text{C}$  pulses),  $72 \mu\text{s}$  (GARP decoupling), and  $600 \mu\text{s}$  (C=O GARP).

ing problem. This, however, also reduces the number of spins that can be observed, decreasing sensitivity. We have taken an alternative route, to use a maximum level of  $^{13}\text{C}$  labeling and to remove the large  $\text{C}_\alpha$ -to-carbonyl couplings by decoupling of the carbonyl resonances.

The pulse sequence used in the present study is shown in Fig. 1. Decoupling of the carbonyl resonances was obtained using an external synthesizer, with a homebuilt X-nucleus decoupling unit, utilizing the GARP (25) sequence. The carbonyl decoupling RF field (400 Hz) was sufficiently weak not to perturb the resonances of the protonated carbons of interest. The experiment was recorded in the fully nonselective mode, observing aromatic and aliphatic resonances simultaneously. A second GARP decoupler unit and 3.2 W RF power (3.3 kHz RF field) were used to decouple aromatic and aliphatic carbons from their directly attached protons during the  $t_1$  and  $t_3$  periods. Spectra were recorded on a Bruker AM500 spectrometer, modified to avoid the wasteful overhead time at the end of every ( $t_1, t_2$ ) increment. The 3D experiment was recorded using 128 and 64 complex data points in the  $t_1$  and  $t_2$  dimensions, respectively, and 512 real points during  $t_3$ . The total measuring time was 2.5 days. Data were processed with software described previously (26). Acquisition times were 32, 8.06, and 51.2 ms in the  $t_1, t_2$ , and  $t_3$  dimension, respectively. Zero filling to yield a digital resolution of 8, 60, and 5 Hz in the  $F_1, F_2$ , and  $F_3$  dimension was used.

Because of the relationship between  $^1\text{H}$  and  $^{13}\text{C}$  chemical shifts (downfield carbons correlate with downfield protons), it is possible to use folding in the  $^{13}\text{C}$  dimension of the 3D spectrum without introducing ambiguity. In the present case, the  $^{13}\text{C}$  spectral window was limited to 63 ppm, with the carrier positioned at 50 ppm. As described previously (26), the  $F_2$  carrier position is moved during data processing in such a manner that all aliphatic resonances fall within the 63 ppm window. The aromatic resonances then appear folded in the  $F_2$  dimension. Because the experiment has been set up to give a  $180^\circ$  linear phase error across the  $F_2$  spectral domain, folded resonances are in phase but of opposite sign relative to the aliphatic resonances (26). Because at a given  $^1\text{H}$  frequency the spectral range of the correlated  $^{13}\text{C}$  resonances never exceeds 40 ppm, an even greater reduction in  $F_2$  spectral width would be possi-

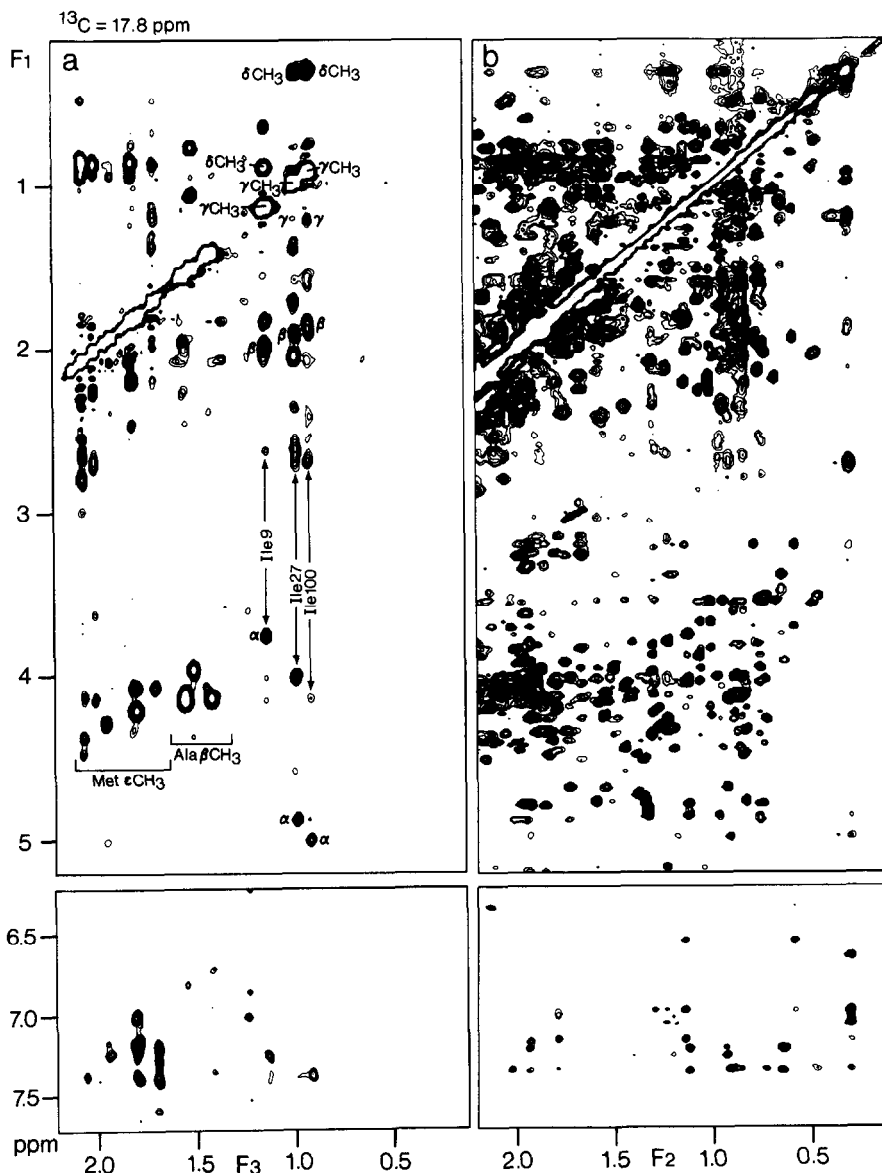


Fig. 2. Comparison of (a) a section of a ( $F_1$ ,  $F_3$ ) slice taken at  $F_2 = 17.8$  ppm from the 500 MHz 3D NOESY-HMQC spectrum, recorded with the pulse sequence of Fig. 1, and (b) the same region of the 600 MHz 2D NOESY spectrum. No baseline correction or other cosmetic procedure has been used in any of the spectra. The 3D spectrum has been recorded at 35°C, p<sup>2</sup>H 6.3, 1.5 mM 95% <sup>13</sup>C-labeled calmodulin, 6.2 mM Ca<sup>2+</sup>. Spectrum (b) has been recorded at 45°C, p<sup>2</sup>H 6.2, 1.5 mM unlabeled calmodulin, 6.2 mM Ca<sup>2+</sup>.

ble without causing accidental overlap between folded and not folded aliphatic resonances.

Spectra have been recorded for a sample of 1.5 mM calmodulin (16.7 kDa), p<sup>2</sup>H 6.3, 6.2 mM Ca<sup>2+</sup>, 35°C, using a 120 ms NOE mixing period. Figure 2 compares part

of a ( $F_1$ ,  $F_3$ ) slice of the 3D spectrum, taken at a  $^{13}\text{C}$  frequency of 17.8 ppm, with the corresponding region of the 2D  $^1\text{H}$  NOESY spectrum, illustrating the dramatic simplification that occurs in the 3D spectrum. NOEs involving methyl groups and other hydrophobic resonances are particularly important for determining the 3D structure of proteins since many of these interactions are long range (between residues more than five amino acids apart in the sequence). Assignments for intraresidue NOEs involving the  $\text{C}_\gamma\text{H}_3$  groups of residues Ile-9, Ile-27, and Ile-100 are indicated in the figure, and it is readily appreciated that these NOE interactions are extremely difficult to identify in the corresponding region of the regular 2D spectrum. Methionine  $\text{C}_\epsilon$  resonances are easily recognized in the high-resolution  $^1\text{H}$ - $^{13}\text{C}$  shift correlation spectrum because of the absence of  $^1J_{\text{CC}}$  splitting, and the corresponding resonances in Fig. 2a are identified. Alanine residues are also easily identified when the results of this 3D experiment are compared with the 3D spectrum obtained with an analogous experiment that provides  $J$  connectivity (data not shown).

The example shown above illustrates the power of the 3D technique to remove overlap in the crowded aliphatic region of the spectrum. A second major strongpoint of the  $^{13}\text{C}$  HMQC-NOESY method stems from its symmetry properties: two protons A and B show NOE cross peaks at ( $A_{\text{H}}$ ,  $B_{\text{C}}$ ,  $B_{\text{H}}$ ) and at ( $B_{\text{H}}$ ,  $A_{\text{C}}$ ,  $A_{\text{H}}$ ), where  $A_{\text{H}}$  and  $B_{\text{H}}$  are the  $^1\text{H}$  frequencies of A and B, and  $A_{\text{C}}$  and  $B_{\text{C}}$  are the frequencies of the carbons directly attached to A and B. This is helpful for making unambiguous assignments of NOE cross peaks, as illustrated in Fig. 3. For example, a resonance A at ( $F_2$ ,  $F_3 = 72.1$ , 3.88 ppm) interacts with a proton B at  $F_1 = 4.04$  ppm (Fig. 3b). About half a dozen protons resonate at  $4.04 \pm 0.02$  ppm. However, by searching the 3D matrix for a cross peak at coordinates (3.88,  $F_2$ , 4.04), the  $^{13}\text{C}$  frequency of A can be established, uniquely identifying A. Figure 3c shows part of the ( $F_1$ ,  $F_3$ ) slice taken at a  $^{13}\text{C}$  frequency of 71.1 ppm, displaying this interaction. The  $^{13}\text{C}$  shifts of A and B strongly suggest that both protons are  $\text{C}_\beta\text{H}$  protons of threonine residues. Further analysis of the 3D NOE spectrum and of  $^{15}\text{N}$  3D NOE-HMQC and HOHAHA-HMQC spectra (unpublished results) proves these resonances to correspond to Thr-26 and Thr-62. In Fig. 3, both  $\text{C}_\beta\text{H}$  resonances show NOEs to their own methyl group. Thr-62  $\text{C}_\beta\text{H}$  also shows an NOE to the methyl resonance of Thr-26. Similarly, the Thr-62 methyl group shows NOEs to both  $\text{C}_\beta\text{H}$  and both  $\text{C}_\alpha\text{H}$  protons (Fig. 3d). Because of extensive overlap in the corresponding regions of the regular 2D NOE spectrum (recorded at 600 MHz) (Fig. 2b), the NOEs mentioned above are not easily identified in such a spectrum.

Elsewhere we will report a novel 3D method that provides  $J$  connectivity between aliphatic resonances, relying on  $J_{\text{CC}}$  connectivity (27). Our preliminary experience with the combined use of these two types of 3D spectra indicates that the analysis of such a pair of 3D spectra is very straightforward, making it particularly easy to distinguish intra- from interresidue interactions. We have demonstrated that heteronuclear  $^1\text{H}$ - $^{13}\text{C}$ - $^1\text{H}$  3D NMR spectroscopy of medium-size proteins is feasible at relatively low sample concentrations (1.5 mM) and in relatively modest amounts of measuring time (2.5 days). The dramatic simplification found earlier for  $^{15}\text{N}$  heteronuclear 3D spectra (10-12) and the relatively high sensitivity of the 3D methods (10, 11) also apply to the  $^{13}\text{C}$  case. The main problem remaining now is the analysis of the tremendous number of NOE interactions found in the 3D spectrum. Because of reduced

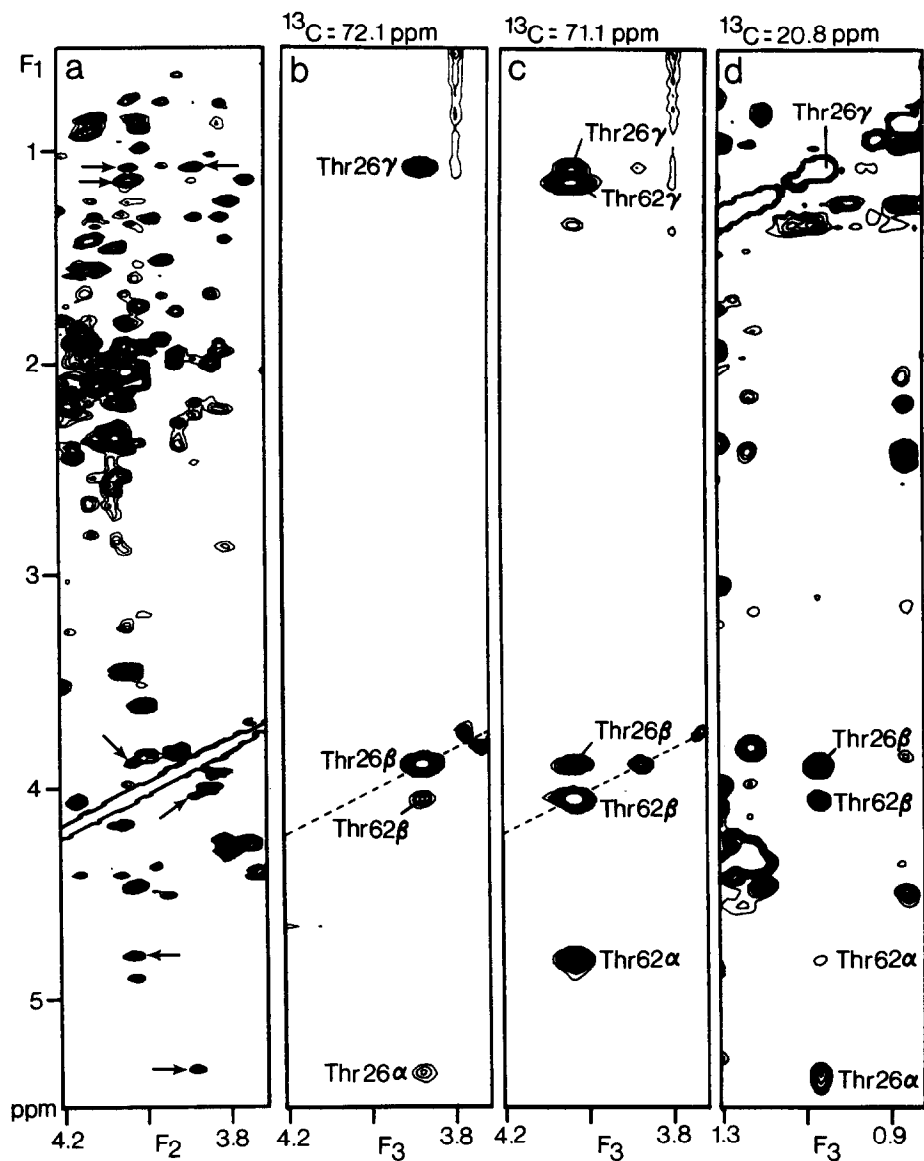


FIG. 3. Comparison of (a) a small region of the 600 MHz 2D NOESY spectrum of calmodulin with (b, c) corresponding regions of slices taken from the 3D spectrum, and (d) a slice showing the interactions with Thr-26- $C_3H_3$ . The labeled resonances in (b) and (c) have been marked by arrows in (a).

overlap present in the 3D spectrum, it is ideally suited for automated analysis and we are currently working on the development of appropriate software for this purpose.

#### ACKNOWLEDGMENTS

We thank Dr. Claude Klee and Marie Krinks for assistance in preparing the sample of calmodulin used in this study, Dr. Kathy Beckingham for providing us with the *Drosophila* calmodulin coding construct,

and Dr. Paul C. Driscoll for useful suggestions during the preparation of this manuscript. This work was supported by the Intramural AIDS Antiviral Program of the Office of the Director of the National Institutes of Health. L.E.K. acknowledges financial support from the Medical Research Council of Canada and the Alberta Heritage Trust Foundation.

## REFERENCES

1. A. BAX AND M. A. WEISS, *J. Magn. Reson.* **71**, 571 (1987).
2. H. SENN, G. OTTING, AND K. WUTRICH, *J. Am. Chem. Soc.* **109**, 1090 (1987).
3. M. RANCE, P. E. WRIGHT, B. A. MESSERLE, AND L. D. FIELD, *J. Am. Chem. Soc.* **109**, 1591 (1987).
4. S. W. FESIK, R. T. GAMPE, AND T. W. ROCKWAY, *J. Magn. Reson.* **74**, 366 (1987).
5. L. P. MCINTOSH, F. W. DAHLQUIST, AND A. G. REDFIELD, *J. Biomol. Struct. Dyn.* **5**, 21 (1987).
6. D. A. TORCHIA, S. W. SPARKS, AND A. BAX, *Biochemistry* **28**, 5509 (1989).
7. D. A. TORCHIA, S. W. SPARKS, P. E. YOUNG, AND A. BAX, *J. Am. Chem. Soc.* **111**, 8315 (1989).
8. H. OSCHKINAT, C. GRIESINGER, P. J. KRAULIS, O. W. SORENSEN, R. R. ERNST, A. M. GRONENBORN, AND G. M. CLORE, *Nature (London)* **332**, 374 (1988).
9. G. W. VUJISTER, R. BOELENS, AND R. KAPTEIN, *J. Magn. Reson.* **80**, 176 (1988).
10. D. MARION, L. E. KAY, S. W. SPARKS, D. A. TORCHIA, AND A. BAX, *J. Am. Chem. Soc.* **111**, 1515 (1989).
11. E. R. P. ZUIDERWEG AND S. W. FESIK, *Biochemistry* **28**, 2387 (1989).
12. D. MARION, P. C. DRISCOLL, L. E. KAY, P. T. WINGFIELD, A. BAX, A. M. GRONENBORN, AND G. M. CLORE, *Biochemistry* **28**, 6150 (1989).
13. S. W. FESIK AND E. R. P. ZUIDERWEG, *J. Magn. Reson.* **78**, 588 (1988).
14. J. JEENER, B. H. MEIER, P. BACHMANN, AND R. R. ERNST, *J. Chem. Phys.* **71**, 4546 (1979).
15. S. MACURA AND R. R. ERNST, *Mol. Phys.* **41**, 95 (1980).
16. L. BRAUNSCHEWEILER AND R. R. ERNST, *J. Magn. Reson.* **53**, 521 (1983).
17. A. BAX AND D. G. DAVIS, *J. Magn. Reson.* **65**, 355 (1985).
18. M. R. BENDALL, D. T. PEGG, AND D. M. DODDRELL, *J. Magn. Reson.* **52**, 81 (1983).
19. A. BAX, R. H. GRIFFEY, AND B. L. HAWKINS, *J. Am. Chem. Soc.* **105**, 7188 (1983).
20. R. H. GRIFFEY, A. G. REDFIELD, R. E. LOOMIS, AND F. W. DAHLQUIST, *Biochemistry* **24**, 817 (1985).
21. A. BAX, M. IKURA, L. E. KAY, D. A. TORCHIA, AND R. TSCHUDIN, *J. Magn. Reson.*, in press.
22. B. H. OH, W. M. WESTLER, P. DARBA, AND J. L. MARKLEY, *Science* **240**, 857 (1988).
23. W. M. WESTLER, M. KAINOSHO, H. NAGAO, N. TOMONAGA, AND J. L. MARKLEY, *J. Am. Chem. Soc.* **110**, 4093 (1988).
24. B. J. STOCKMAN, M. D. REILY, W. M. WESTLER, E. L. ULRICH, AND J. L. MARKLEY, *Biochemistry* **28**, 230 (1989).
25. A. J. SHAKA, P. B. BARKER, AND R. FREEMAN, *J. Magn. Reson.* **64**, 547 (1985).
26. L. E. KAY, D. MARION, AND A. BAX, *J. Magn. Reson.* **84**, 72 (1989).
27. L. E. KAY, M. IKURA, AND A. BAX, *J. Am. Chem. Soc.*, in press.